

Tomography of the Earth's Core Using Supernova Neutrinos

Manfred Lindner^{a*}, Tommy Ohlsson^{ab†}, Ricard Tomàs^{c‡}, Walter Winter^{a§}

^a*Institut für Theoretische Physik, Physik-Department, Technische Universität München, James-Franck-Straße, 85748 Garching bei München, Germany*

^b*Division of Mathematical Physics, Department of Physics, Royal Institute of Technology (KTH) - Stockholm Center for Physics, Astronomy, and Biotechnology, 106 91 Stockholm, Sweden*

^c*Max-Planck-Institut für Physik (Werner-Heisenberg-Institut), Föhringer Ring 6, 80805 München, Germany*

Abstract

We investigate the possibility to use the neutrinos coming from a future galactic supernova explosion to perform neutrino oscillation tomography of the Earth's core. We propose to use existing or planned detectors, resulting in an additional payoff. Provided that all of the discussed uncertainties can be reduced as expected, we find that the average matter densities of the Earth's inner and outer cores could be measured with a precision competitive with geophysics. However, since seismic waves are more sensitive to matter density jumps than average matter densities, neutrino physics would give partly complementary information.

PACS: 14.60.Lm; 13.15.+g; 91.35.-x; 97.60.Bw

Key words: Neutrino oscillations; Supernova neutrinos; Neutrino tomography; Geophysics

1. Introduction

In order to obtain more information about the interior of the Earth, neutrino tomography has been considered as an alternative method to geophysics. There exist, in principle, two different such techniques, neutrino absorption tomography [1, 2, 3, 4, 5, 6, 7, 8, 9] and neutrino oscillation tomography [10, 11, 12, 13, 14]. Neutrino absorption tomography, based on the absorption of neutrinos in matter, is in some sense similar to X-ray tomography and unfortunately faces several problems including the need of extremely high energetic neutrino sources, huge detectors, and the prerequisite of many baselines. Neutrino oscillation tomography uses the fact that neutrino oscillations are influenced by the presence of matter [15, 16, 17]. Neutrino oscillation tomography would, in principle, be possible with a single baseline, since interference effects provide additional information on the matter density

profile. However, it requires quite precise knowledge about the neutrino oscillation parameters and stringent bounds on the contribution of non-oscillation physics, such as neutrino decay, CPT violation, non-standard interactions, sterile neutrinos, *etc.* Supernovae as neutrino sources are especially interesting, since the neutrinos come in large numbers from a short burst, which could be used to obtain a snapshot of the Earth's interior. In addition, compared to solar neutrinos, their energy spectrum has a high-energy tail, which is more sensitive to Earth matter effects. The influence of Earth matter on supernova neutrinos has, for example, been studied in Refs. [18, 19, 20].

We assume that technologically feasible detectors exist, such as Super-Kamiokande, SNO, Hyper-Kamiokande, and UNO, which are originally built for different purposes, but also capable to detect supernova neutrinos. We discuss the possibility to use the neutrinos coming from a future galactic supernova explosion to determine with the assumed detectors some of the measurable quantities describing the structure of the Earth's interior. We especially focus on the outer and inner core of the Earth, since they are

*E-mail: lindner@ph.tum.de

†E-mail: tohlsson@ph.tum.de, tommy@theophys.kth.se

‡E-mail: ricard@mppmu.mpg.de

§E-mail: wwinter@ph.tum.de

much harder to access with conventional geophysical methods than the mantle of the Earth.

2. Geophysical aspects

In geophysics, the most promising technique to access the Earth’s interior is to use seismic wave propagation (for a summary, see Refs. [21, 22]). Especially, the detection of seismic waves produced by earthquakes gives valuable information on the seismic wave velocity profile of the Earth matter. However, the matter density is not directly accessible, but indirectly obtained by assumptions about the equation of state of the considered materials. Since seismic S-waves are mainly reflected at the mantle-core boundary, information on the Earth’s core is much harder to obtain than on the Earth’s mantle. Therefore, we will especially focus on the Earth’s core in this paper. Since reflection and refraction of P-waves at transition boundaries with large matter density contrasts are quite easy to observe with seismic waves, the mantle-core and outer core-inner core boundaries can be located with high precision as well as the matter density jumps can be measured. For example, the matter density jump at the outer core-inner core boundary is often given by $(0.55 \pm 0.05) \text{ g/cm}^3$ [23]. This is quite a difference compared to neutrino physics, since neutrino oscillations in matter are especially sensitive to the average matter densities (on the scale of the neutrino oscillation length) indirectly measured by the electron density. Thus, neutrino oscillations are less sensitive to local differences, but they involve less unknowns from the equation of state and could therefore access the absolute matter densities instead of the matter density jumps.

Several issues regarding the Earth’s inner core are considered to be interesting from a geophysical point of view. For different indirect reasons the inner core is believed to consist mainly of iron and it is therefore often called the iron core. First of all, the spectral lines in the sunlight indicate that the atmosphere of the Sun partly consists of iron as a potential material source for the planets. A second hint comes from the magnetic field of the Earth. After all, there are no convincing alternatives. We will see later that neutrino to-

mography could directly verify the average matter density of an iron core. Further topics relevant for the inner core structure are: anisotropy, heterogeneity, time-dependence, solidity, and rotation (for a summary, see Ref. [24]). However, since neutrino oscillations are to a good approximation only sensitive to average matter densities at long scales, these issues are much harder to access with neutrino oscillation tomography.

3. Core-collapse supernovae as neutrino sources

Core-collapse supernovae represent the evolutionary end of massive stars with a mass $M \gtrsim 8M_\odot$, where M_\odot is the mass of the Sun. In these explosions, about 99 % of the liberated gravitational binding energy, $E_b \simeq 3 \cdot 10^{53} \text{ erg}$, is carried away by neutrinos in roughly equal amounts of energy for all flavors in the first 10 seconds after the onset of the core collapse [25]. It is widely believed that the time-dependent energy spectrum of each neutrino species can be approximated by a “pinched” Fermi–Dirac distribution [26, 27, 28]. In this work, we assume that the time-integrated spectra can also be well approximated by the pinched Fermi–Dirac distributions with an effective degeneracy parameter η , *i.e.*,

$$N_\nu^0(E) = \frac{E_\nu^{\text{tot}}}{\langle E_\nu \rangle} \frac{1}{F_2(\eta) T^3} \frac{E^2}{e^{E/T-\eta} + 1}, \quad (1)$$

where $E_\nu^{\text{tot}} \equiv \int L_\nu dt$ is the total neutrino energy of a certain flavor ν ,

$$F_k(y) \equiv \int_0^\infty \frac{x^k}{e^{x-y} + 1} dx,$$

and E and T denote the neutrino energy and the effective temperature, respectively. The relation between the average neutrino energy and the effective neutrino temperature is given by

$$\langle E_\nu \rangle = \frac{\int_0^\infty E N_\nu^0 dE}{\int_0^\infty N_\nu^0 dE} = \frac{F_3(\eta)}{F_2(\eta)} T. \quad (2)$$

In this section, we assume for simplicity that $\eta = 0$ for all neutrino flavors¹, which means that

$$\langle E_\nu \rangle = \frac{F_3(0)}{F_2(0)} T = \frac{7\pi^4}{180\zeta(3)} T \equiv kT, \quad (3)$$

where $\zeta(x)$ is the Riemann z-function [$\zeta(3) \simeq 1.20206$] and $k \simeq 3.15137$. Furthermore, the time-integrated flux of the neutrinos can be expressed by

$$\Phi_\nu^0 = \frac{N_\nu^0}{4\pi D^2}, \quad (4)$$

where D is the distance to the supernova.

Due to the different trapping processes, the different neutrino flavors originate in layers of the supernova with different temperatures. The electron (anti)neutrino flavor is kept in thermal equilibrium by β processes up to a certain radius usually referred to as the “neutrinosphere”, beyond which the neutrinos stream off freely. However, the practical absence of muons and taus in the supernova core implies that the other two neutrino flavors, here collectively denoted by ν_x ($\nu_\mu, \nu_\tau, \bar{\nu}_\mu, \bar{\nu}_\tau$), interact primarily by less efficient neutral-current processes. Therefore, their spectra are determined at deeper, *i.e.*, hotter, regions. In addition, since the content of neutrons is larger than that of protons, ν_e 's escape from outer regions than $\bar{\nu}_e$'s. This rough picture leads to the following hierarchy: $\langle E_{\nu_e} \rangle < \langle E_{\bar{\nu}_e} \rangle < \langle E_{\nu_x} \rangle$. Here ν_x refers again to both ν_μ and ν_τ . Typical values of the average energies of the time-integrated neutrino spectra obtained in simulations are $\langle E_{\nu_e} \rangle \sim 12$ MeV, $\langle E_{\bar{\nu}_e} \rangle \sim 15$ MeV, and $\langle E_{\nu_x} \rangle \sim 24$ MeV [30,31]. However, recent studies with an improved treatment of neutrino transport, microphysics, the inclusion of the nucleon bremsstrahlung, and the energy transfer by recoils, find somewhat smaller differences between the $\bar{\nu}_e$ and ν_x spectra [32,33].

In the following, we assume a future galactic supernova explosion at a typical distance of $D = 10$ kpc, with a binding energy of $E_b = 3 \cdot 10^{53}$ erg

¹In the analysis, we will also show some results for $\eta_{\bar{\nu}_e} = 3$ and $\eta_{\bar{\nu}_\mu} = 1$ [29]. The extension of the formulas to these cases are quite straightforward, though making them more complicated.

Scenario	ξ	τ_E	$\eta_{\bar{\nu}_e}$	$\eta_{\bar{\nu}_\mu}$
S1	1	1.4	0	0
S2	1	1.2	0	0
S3	0.5	1.4	0	0
S4	0.5	1.2	0	0
S5	1.2	1.4	0	0
S6	1.2	1.2	0	0
S7	1	1.4	3	1
S8	1	1.2	3	1
S9	1.2	1.4	3	1
S10	1.2	1.2	3	1

Table 1

Our standard scenarios for supernova parameters, where in all cases $\langle E_{\bar{\nu}_e} \rangle = 15$ MeV.

and a total energy of $E_{\nu_e}^{\text{tot}} = E_{\bar{\nu}_e}^{\text{tot}} \equiv E_{\nu_x}^{\text{tot}}/\xi$, where ξ parameterizes a possible deviation from energy equipartition [34]. We also assume that the fluxes of ν_μ , ν_τ , $\bar{\nu}_\mu$, and $\bar{\nu}_\tau$ are identical and we fix $\langle E_{\bar{\nu}_e} \rangle$ to 15 MeV. Due to the current lack of a standard picture of core-collapse supernovae we consider for our analysis six scenarios for $\eta = 0$ with different values of the parameters $\tau_E \equiv \langle E_{\bar{\nu}_x} \rangle / \langle E_{\bar{\nu}_e} \rangle \in \{1.2, 1.4\}$ and $\xi \in \{0.5, 1, 1.2\}$, as shown in Tab. 1. In addition, we study four scenarios with $\eta_{\bar{\nu}_e} = 3$ and $\eta_{\bar{\nu}_\mu} = 1$ as well as $\tau_E \in \{1.2, 1.4\}$ and $\xi \in \{1, 1.2\}$.

As far as the neutrino detection is concerned, we only analyze the charged-current reaction $\bar{\nu}_e + p \rightarrow e^+ + n$, since this reaction yields the largest number of events (around 8000 in the Super-Kamiokande detector in the case of a galactic supernova). Therefore, we shall concentrate on the study of the propagation of antineutrinos from a supernova to detectors on the Earth. The cross section details for the reaction $\bar{\nu}_e + p \rightarrow e^+ + n$ can be found and are discussed in Ref. [35].

4. From neutrino production to neutrino detection

In general, neutrino propagation from a source to a detector is described by an evolution operator on the form

$$\mathcal{U} \equiv \mathcal{U}(L) = e^{-i \int_0^L \mathcal{H}(L') dL'}, \quad (5)$$

where the exponential function is time-ordered, $\mathcal{H} \equiv \mathcal{H}(L)$ is the total Hamiltonian and L is the neutrino (traveling) path length, *i.e.*, the baseline length. The Hamiltonian is usually given either in the flavor basis or in the mass basis. In the flavor basis, the total Hamiltonian reads $\mathcal{H}_f(L) = UH_mU^{-1} + A(L)\text{diag}(1, 0, 0)$, where $H_m \equiv \text{diag}(E_1, E_2, E_3)$ is the free Hamiltonian in the mass basis, $U \equiv (U_{\alpha a})$ is the leptonic mixing matrix, and

$$A \equiv A(L) = \pm\sqrt{2}G_F\frac{Y_e}{m_N}\rho(L) \quad (6)$$

is the mass density parameter related to the matter density $\rho \equiv \rho(L)$. Here $E_a \equiv m_a^2/(2E)$ ($a = 1, 2, 3$), $G_F \simeq 1.16639 \cdot 10^{-23} \text{eV}^{-2}$ is the Fermi weak coupling constant, Y_e is the average number of electrons per nucleon², and $m_N \simeq 939 \text{MeV}$ is the nucleon mass. The sign depends on the presence of neutrinos (+) or antineutrinos (-). Furthermore, m_a is the mass of the a th mass eigenstate ν_a and E is the neutrino energy. In order to obtain the neutrino oscillation transition probabilities, we need to calculate the matrix elements of the evolution operator in the flavor basis, take the absolute values of these, and then square them. The neutrino oscillation probability amplitude from a neutrino flavor ν_α to a neutrino flavor ν_β is defined as

$$A_{\alpha\beta} \equiv \langle \nu_\beta | \mathcal{U}_f(L) | \nu_\alpha \rangle, \quad \alpha, \beta = e, \mu, \tau, \quad (7)$$

where \mathcal{U}_f is the total evolution operator in the flavor basis. Then, the neutrino oscillation transition probability for $\nu_\alpha \rightarrow \nu_\beta$ is given by

$$P_{\alpha\beta} \equiv |A_{\alpha\beta}|^2, \quad \alpha, \beta = e, \mu, \tau. \quad (8)$$

The initial neutrino fluxes arise from the central part of the supernova, where the matter density is of the order of about 10^{12}g/cm^3 . For such high matter densities one can infer from the expression of the Hamiltonian \mathcal{H}_f that the matter mass eigenstates, ν_a^m ($a = 1, 2, 3$), coincide with the flavor states, ν_α ($\alpha = e, \mu, \tau$), up to a rotation between ν_μ and ν_τ . Thus, in the case of normal mass hierarchy, $m_1 \lesssim m_2 \ll m_3$, one has

$$\underline{\bar{\nu}_1^m = \bar{\nu}_e, \quad \bar{\nu}_2^m = \bar{\nu}'_\mu, \quad \bar{\nu}_3^m = \bar{\nu}'_\tau}, \quad (9)$$

²In the Earth: $Y_e \simeq \frac{1}{2}$.

where $\bar{\nu}'_\mu$ and $\bar{\nu}'_\tau$ are the rotated states. Therefore, one can assume that the original fluxes of the matter mass eigenstates are³

$$\Phi_{\bar{\nu}_1^m}^0 = \Phi_{\bar{\nu}_e}^0, \quad \Phi_{\bar{\nu}_2^m}^0 = \Phi_{\nu_x}^0, \quad \Phi_{\bar{\nu}_3^m}^0 = \Phi_{\nu_x}^0. \quad (10)$$

Since we are assuming that $\bar{\nu}_\mu$ and $\bar{\nu}_\tau$ have the same fluxes, the neutrino transitions are determined by the mixings of the $\bar{\nu}_e$ only, *i.e.*, by U_{ea} [37]. Moreover, under the assumption of normal mass hierarchy, antineutrinos do not undergo any resonant conversion, which means that the small mixing angle θ_{13} is suppressed in matter and the $\bar{\nu}_e \leftrightarrow \bar{\nu}_3$ transitions are negligible. One consequence is that $\bar{\nu}_3^m$ propagates adiabatically and leaves the supernova as $\bar{\nu}_3$. The propagation of the other two states depends on the parameters of the solution to the solar neutrino problem and it may be adiabatic or non-adiabatic [38, 39]. In particular, we will focus on the Mikheyev–Smirnov–Wolfenstein (MSW) [15, 16, 17] large mixing angle (LMA) solution, since it is by far the most favored one. For the parameters within such a region the neutrino evolution through the supernova (SN) envelope is adiabatic. Thus, $\bar{\nu}_e$ will leave the supernova as $\bar{\nu}_1$, $\bar{\nu}'_\mu$ as $\bar{\nu}_2$, and $\bar{\nu}'_\tau$ as $\bar{\nu}_3$. Finally, the measured fluxes of supernova neutrinos at a detector on the Earth are

$$\Phi_{\nu_\alpha} = \sum_{a=1}^3 P_{a\alpha} \Phi_{\nu_a}^0, \quad \alpha = e, \mu, \tau, \quad (11)$$

where $\Phi_{\nu_a}^0$ ($a = 1, 2, 3$) are the initial supernova neutrino fluxes.

For neutrino propagation from a supernova (SN core) to a detector at the Earth (see Fig. 1) we have the probability amplitudes

$$\begin{aligned} A_{\alpha\beta} &= \langle \nu_\beta | \mathcal{U}_f^{\text{tot}}(L) | \nu_\alpha \rangle \\ &= \langle \nu_\beta | \mathcal{U}^\oplus(L_\oplus) \mathcal{U}^{\text{vac}}(L_{\text{vac}}) \mathcal{U}^{\text{SN}}(L_{\text{SN}}) | \nu_\alpha \rangle, \end{aligned} \quad (12)$$

³Any rotation between $\bar{\nu}_\mu$ and $\bar{\nu}_\tau$ does not affect the corresponding total mass eigenstate contents, because they have the same fluxes, as discussed in the last section. For an analysis taking into account possible differences in the fluxes, see Ref. [36]. In addition, an argument against neutrino oscillations between $\bar{\nu}_\mu$ and $\bar{\nu}_\tau$ on their way to the Earth will be given at the end of this section.

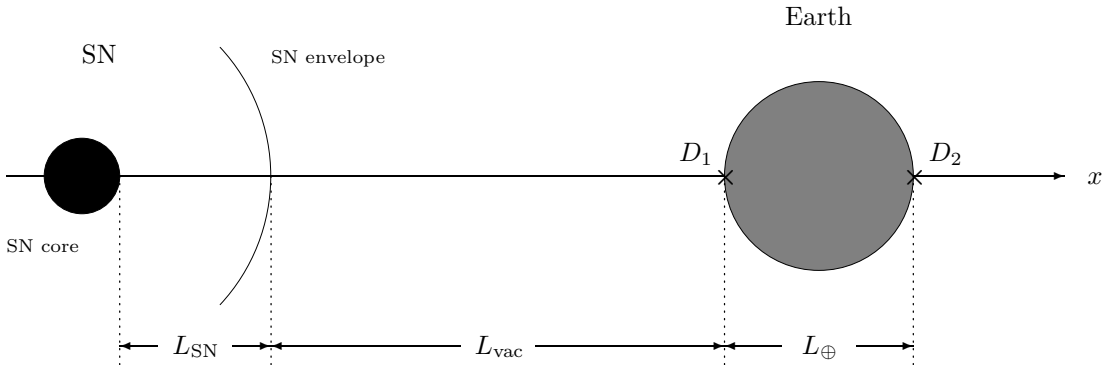


Figure 1. The propagation of neutrinos from a supernova (SN) to the Earth. The detector D_1 can be anywhere on the Earth's side towards the SN, whereas the detector D_2 should be in the shadow of the Earth's core.

where \mathcal{U}^{SN} , \mathcal{U}^{vac} , and \mathcal{U}^{\oplus} are the evolution operators in the supernova (from SN core to SN envelope), in vacuum, and in the Earth, respectively, and L_{SN} , L_{vac} , and L_{\oplus} are the corresponding baseline lengths. Note that the operators \mathcal{U}^{SN} , \mathcal{U}^{vac} , and \mathcal{U}^{\oplus} in general do not commute. Using the completeness relation, one can write the probability amplitudes as

$$A_{\alpha\beta} = \sum_{a=1}^3 \langle \nu_{\beta} | \mathcal{U}^{\oplus}(L_{\oplus}) \mathcal{U}^{\text{vac}}(L_{\text{vac}}) | \nu_a \rangle \times \langle \nu_a | \mathcal{U}^{\text{SN}}(L_{\text{SN}}) | \nu_{\alpha} \rangle. \quad (13)$$

Since we have seen that for adiabatic transitions the supernova neutrinos leave the supernova (SN envelope) as neutrino mass eigenstates ν_a , *i.e.*, $\langle \nu_a | \mathcal{U}^{\text{SN}}(L_{\text{SN}}) | \nu_{\alpha} \rangle = \delta_{\alpha a}$, we can re-define the probability amplitudes

$$A_{a\alpha} \equiv \langle \nu_{\alpha} | \mathcal{U}^{\oplus}(L_E) \mathcal{U}^{\text{vac}}(L_{\text{vac}}) | \nu_a \rangle, \quad (14)$$

where the first index is a mass eigenstate index ($a = 1, 2, 3$) and the second index is a flavor state index ($\alpha = e, \mu, \tau$). These “mixed” probability amplitudes will completely determine the evolution of the neutrinos from a supernova (SN envelope) to the Earth. Now, there are, in principle, two cases for a supernova neutrino to be detected at the Earth (see again Fig. 1):

1. The supernova neutrino arrives at the detector from above, *i.e.*, it does not go through the Earth at all (detector D_1).
2. The supernova neutrino goes through the Earth's and then arrives at the detector (detector D_2).

Let us start with the first case. The probability amplitude for an initial neutrino mass eigenstate ν_a , where $a = 1, 2, 3$, to leave the supernova and to convert into a flavor state ν_{α} , where $\alpha = e, \mu, \tau$, is at the detector D_1 formally defined as

$$A_{a\alpha}^{D_1} = \langle \nu_{\alpha} | \mathcal{U}^{\text{vac}}(L_{\text{vac}}) | \nu_a \rangle. \quad (15)$$

Note that we assumed that a neutrino mass eigenstate ν_a left the supernova, and therefore, no evolution operator \mathcal{U}^{SN} should appear in the above equation. Furthermore, since the supernova neutrino does not go through the Earth, there appears also no evolution operator \mathcal{U}^{\oplus} in this equation. Next, since the evolution operator in vacuum \mathcal{U}^{vac} is diagonal in the mass basis, we find

that Eq. (15) reduces to⁴

$$\begin{aligned} A_{a\alpha}^{D_1} &= \langle \nu_\alpha | \nu_a \rangle = \sum_{b=1}^3 U_{\alpha b} \langle \nu_b | \nu_a \rangle \\ &= \sum_{b=1}^3 U_{\alpha b} \delta_{ab} = U_{\alpha a}, \end{aligned} \quad (16)$$

i.e., the probability amplitudes are just the matrix elements of the leptonic mixing matrix. Thus, we have $P_{a\alpha}^{D_1} = |A_{a\alpha}^{D_1}|^2 = |U_{\alpha a}|^2$, and inserting this into Eq. (11), we obtain the supernova neutrino fluxes at the detector D_1 as

$$\Phi_{\nu_\alpha}^{D_1} = \sum_{a=1}^3 |U_{\alpha a}|^2 \Phi_{\nu_a}^0, \quad \alpha = e, \mu, \tau. \quad (17)$$

Assuming as in Eq. (10) that the initial fluxes of the second and third mass eigenstates are equal, *i.e.*, $\Phi_{\bar{\nu}_2}^0 = \Phi_{\bar{\nu}_3}^0$, the electron antineutrino flux at the detector D_1 can be written as

$$\Phi_{\bar{\nu}_e}^{D_1} = \Phi_{\bar{\nu}_1}^0 [|U_{e1}|^2 + f_R (|U_{e2}|^2 + |U_{e3}|^2)]. \quad (18)$$

Here $f_R \equiv \Phi_{\bar{\nu}_2}^0 / \Phi_{\bar{\nu}_1}^0 = \Phi_{\bar{\nu}_3}^0 / \Phi_{\bar{\nu}_1}^0$ is the so-called flux ratio, which is plotted for several values of ξ and τ_E (introduced in the last section) in Fig. 2. Furthermore, the flux ratio f_R depends on the supernova parameters $\langle E_{\bar{\nu}_e} \rangle$, ξ , and τ_E only and reads for $\eta = 0$ ⁵

$$f_R = \frac{\xi}{\tau_E^4} \frac{e^{k \frac{E}{\langle E_{\bar{\nu}_e} \rangle}} + 1}{e^{k \frac{E}{\langle E_{\bar{\nu}_e} \rangle} \tau_E^{-1}} + 1}, \quad (19)$$

where again $k \simeq 3.15137$. Reinserting the probabilities $P_{ae}^{D_1}$ instead of the probability amplitudes U_{ea} in Eq. (18) and using the unitarity condition $P_{1e}^{D_1} + P_{2e}^{D_1} + P_{3e}^{D_1} = 1$, we find that

$$\Phi_{\bar{\nu}_e}^{D_1} = \Phi_{\bar{\nu}_1}^0 P_{1e}^{D_1} \left(1 + f_R \frac{1 - P_{1e}^{D_1}}{P_{1e}^{D_1}} \right), \quad (20)$$

which means that the flux of electron antineutrinos at the detector D_1 is only depending on the

⁴The neutrino flavor states are defined as follows: $|\nu_\alpha\rangle = \sum_{a=1}^3 U_{\alpha a}^* |\nu_a\rangle$ ($\alpha = e, \mu, \tau$), which implies that $\langle \nu_\alpha | = \sum_{a=1}^3 U_{\alpha a} \langle \nu_a |$. Here the $U_{\alpha a}$'s are the matrix elements of the leptonic mixing matrix U .

⁵For $\eta \neq 0$ this equation would be slightly more complicated, but could be easily obtained from Eq. (1).

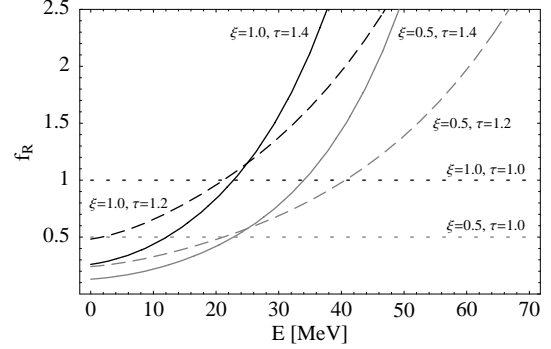


Figure 2. The flux ratio f_R as a function of the neutrino energy E for different values of the parameters ξ and τ_E and for $\eta = 0$, partly corresponding to the scenarios in Tab. 1.

initial neutrino flux $\Phi_{\bar{\nu}_1}^0$, the transition probability $P_{1e}^{D_1} = |U_{e1}|^2$, and the flux ratio f_R .

Next, let us discuss the second case. Again using the fact that the evolution operator in vacuum \mathcal{U}^{vac} is diagonal in the mass basis, we find that

$$\begin{aligned} A_{a\alpha}^{D_2} &= \langle \nu_\alpha | \mathcal{U}^\oplus(L_\oplus) \mathcal{U}^{\text{vac}}(L_{\text{vac}}) | \nu_a \rangle \\ &= \sum_{b=1}^3 \langle \nu_\alpha | \mathcal{U}^\oplus(L_\oplus) | \nu_b \rangle \langle \nu_b | \mathcal{U}^{\text{vac}}(L_{\text{vac}}) | \nu_a \rangle \\ &= \sum_{b=1}^3 \langle \nu_\alpha | \mathcal{U}^\oplus(L_\oplus) | \nu_b \rangle \delta_{ab} \\ &= \langle \nu_\alpha | \mathcal{U}^\oplus(L_\oplus) | \nu_a \rangle = A_{a\alpha}^\oplus. \end{aligned} \quad (21)$$

Similar to the first case, we obtain the supernova neutrino fluxes at the detector D_2 as

$$\Phi_{\nu_\alpha}^{D_2} = \sum_{a=1}^3 |A_{a\alpha}^\oplus|^2 \Phi_{\nu_a}^0, \quad \alpha = e, \mu, \tau, \quad (22)$$

which for the electron antineutrino flux at the detector D_2 can be written as

$$\Phi_{\bar{\nu}_e}^{D_2} = \Phi_{\bar{\nu}_1}^0 P_{1e}^{D_2} \left(1 + f_R \frac{1 - P_{1e}^{D_2}}{P_{1e}^{D_2}} \right). \quad (23)$$

This means that the flux of electron antineutrinos at the detector D_2 depends only on the initial neutrino flux $\Phi_{\bar{\nu}_1}^0$, the transition probability $P_{1e}^{D_2} = |A_{1e}^{D_2}|^2$, and the flux ratio f_R .

Now, we want to determine the neutrino oscillation transition probabilities. Using the evolution operator method developed in Ref. [40], the evolution operator in the Earth, which we will assume to consist of N different (constant) matter density layers, is given by

$$\begin{aligned} \mathcal{U}^\oplus(L_\oplus) &= \mathcal{U}^\oplus(L_N; A_N)\mathcal{U}^\oplus(L_{N-1}; A_{N-1})\dots \\ &\times \mathcal{U}^\oplus(L_2; A_2)\mathcal{U}^\oplus(L_1; A_1) \\ &\equiv \prod_{k=1}^N \mathcal{U}^\oplus(L_k; A_k), \end{aligned} \quad (24)$$

where $\mathcal{U}^\oplus(L_k; A_k) \equiv e^{-i\mathcal{H}(A_k)L_k}$ is the evolution operator in the k th layer with constant matter density and $L_\oplus \equiv \sum_{k=1}^N L_k$.⁶ Here L_k and A_k are the thickness and matter density parameters of the k th matter density layer, respectively. Note again that the evolution operators in the different layers normally do not commute. Inserting Eq. (24) into Eq. (21) and the result thereof into $P_{a\alpha}^{D_2} = |A_{a\alpha}^{D_2}|^2$, we finally obtain

$$P_{a\alpha}^{D_2} = \left| \langle \nu_\alpha | \prod_{k=1}^N \mathcal{U}^\oplus(L_k; A_k) | \nu_a \rangle \right|^2, \quad (25)$$

which is our main formula for the neutrino oscillation transition probabilities from a supernova to the detector D_2 . Thus, inserting $a = 1$ and $\alpha = e$ into Eq. (25), we find the probability $P_{1e}^{D_2}$, which can then be inserted into Eq. (23).

In Fig. 3, we show for the scenario S1 in Tab. 1 the different binned energy spectra at Super-Kamiokande-like detectors, where the solid curve represents the detector D_2 and the dashed curve the detector D_1 . One can easily see that matter effects are largest for energies above about 25 MeV. For a detailed discussion of Earth matter effects of supernova neutrinos, see Refs. [18,19,20] and references therein. In summary, for our chosen values of the neutrino oscillation parameters (MSW LMA solution, maximal atmospheric mixing, and normal mass hierarchy) the relative size of the Earth matter effects increases with energy

⁶Similar applications of the evolution operator for propagation of neutrinos in matter consisting of two density layers using two neutrino flavors have been discussed in Refs. [41,42,43].

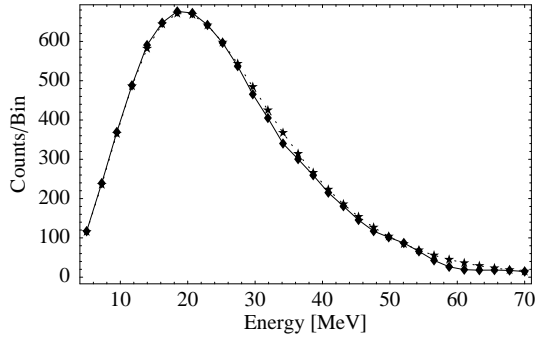


Figure 3. The charged-current events per energy bin from electron antineutrinos in an Super-Kamiokande-like detector for a realistic energy resolution [44]. The solid curve shows the spectrum (scenario S1 in Tab. 1) including the Earth matter effects for a baseline of about 12,700 km through the Earth's core, whereas the dashed curve shows the spectrum without Earth matter effects. The differences appear to be small, but are nevertheless statistically significant, *i.e.*, $\Delta\chi^2 \simeq 35$. Assuming that the matter effects can (approximately) be described by two parameters, such as the average mantle and core densities, this corresponds to at least a 5σ effect. To establish the Earth matter effects at a 3σ confidence level, one would need at least 11 kt fiducial mass detectors. For the neutrino oscillation parameters we used $\theta_{12} = 32.9^\circ$, $\theta_{13} = 5^\circ$, $\theta_{23} = 45^\circ$, $\Delta m_{21}^2 = 5.0 \cdot 10^{-5} \text{ eV}^2$, $\Delta m_{32}^2 = 2.5 \cdot 10^{-3} \text{ eV}^2$, and $\delta_{\text{CP}} = 0$, *i.e.*, a normal mass hierarchy.

and can be seen as oscillatory modulation of the energy spectrum. For small energies, however, this modulation oscillates too fast to be resolved, *i.e.*, it averages out. For large energies about 25 MeV, the frequency becomes smaller and this modulation can be resolved. In Fig. 3, we used the scenario S1 from Tab. 1, making it possible that the fluxes of ν_x dominate above the critical energy around 25 MeV. This results in a negative modulation of the electron antineutrino spectrum, *i.e.*, regeneration effects of $\bar{\nu}_\mu$ and $\bar{\nu}_\tau$, as it is shown in Ref. [18]. However, a general suppression of the fluxes of the ν_x is possible for a value $\xi < 1$, which means that the modulation

can be positive. From Fig. 3, it is also interesting to observe that solar neutrinos show much smaller Earth matter effects (day-night), since the spectrum is cut off far below 25 MeV. Thus, especially the high-energy tail in the supernova neutrino spectrum can make this application possible compared with solar neutrinos.

Let us now go back to Fig. 2, which shows the flux ratio f_R of the ν_x and $\bar{\nu}_1$ fluxes at the surface of the Earth for some of the supernova parameter scenarios in Tab. 1. With Eqs. (1), (19), and (23) as well as this figure, we can estimate the sensitivity for different sets of supernova parameters. This equation describes the flux at the detector D_2 and depends on three different quantities $\Phi_{\bar{\nu}_1}^0$, f_R , and $P_{1e}^{D_2}$. First, the flux $\Phi_{\bar{\nu}_1}^0$ can be indirectly determined by the detector D_1 , since it also appears in Eq. (20) as the enveloping function, *i.e.*, both fluxes $\Phi_{\bar{\nu}_e}^{D_1}$ and $\Phi_{\bar{\nu}_e}^{D_2}$ are directly proportional to $\Phi_{\bar{\nu}_1}^0$. Second, in general, the flux ratio f_R depends on the supernova parameters ξ and τ_E as well as the η 's, which can, up to a certain precision, also be reconstructed from the spectrum at the detector D_1 (*cf.*, discussion in Sec. 7 and Refs. [45, 46]). Note that it could be directly measured if one were also able to detect flavors other than the electron antineutrino, and the supernova parameters would completely drop out (*cf.*, Eq. (17)). Third, the transition probability $P_{1e}^{D_2}$ contains the information about the Earth matter and is usually quite large. Thus, the ratio $(1 - P_{1e}^{D_2})/P_{1e}^{D_2}$ in Eq. (23) is rather sensitive to changes in the Earth matter effects. Since this factor is multiplied with f_R , the energy-dependent flux ratio can enhance or suppress it. Finally, we have also noticed above that the (relative) Earth matter effects are increasing with energy. For the supernova parameters we can then distinguish four different cases, where some of those can also be found in Fig. 2:

1. $\xi = 1$, $\tau_E = 1$, $\eta_{\bar{\nu}_e} = \eta_{\bar{\nu}_\mu} = 0$ (energy equipartition and equal temperatures for all flavors): The flux ratio f_R is equal to unity (*cf.*, Eq. (19)). Then, the neutrino transition probabilities in Eq. (23) drop out and we cannot use the supernova neutrinos for Earth matter effects.
2. $\xi = 1$, $\tau_E > 1$, $\eta_{\bar{\nu}_e} = \eta_{\bar{\nu}_\mu} = 0$ (energy equipartition and a lower temperature for $\bar{\nu}_e$ than for ν_x): The flux ratio f_R is enhanced for large energies, where Earth matter effects are large. The larger τ_E is, the larger becomes this effect. Thus, the scenario S2 in Tab. 1 performs worse than the scenario S1.
3. $\xi \ll 1$ (more electron antineutrinos produced than the other two flavors): The flux ratio $f_R \propto \xi$ is suppressed in general. Therefore, the scenarios S3 and S4 are not as good for our application as the scenario S1.
4. $\tau_E > 1$ and $\xi > 1$ or $\eta_{\bar{\nu}_e} \neq \eta_{\bar{\nu}_\mu}$ (more muon/tau antineutrinos produced than electron antineutrinos or different degeneracy parameters for the different flavors): The flux ratio f_R becomes even steeper than the one for S1, reflecting the more different behavior of the different flavors. Thus, we expect that the scenarios S5 to S10 in Tab. 1 perform much better than the scenario S1, while the optimal scenario should be S9 having the largest ξ and τ_E .

Thus, the larger ξ and τ_E are and the more different $\eta_{\bar{\nu}_e}$ and $\eta_{\bar{\nu}_\mu}$ are, the better our proposed application should work. However, the actual values of these parameters will not be known for sure before the next supernova explodes. Therefore, we choose further on the scenario S1 for reference, which has quite plausible parameter values and will turn out to be a possible model that perfectly illustrates our procedure. In addition, we will summarize the performance of the other scenarios in short form.

For our application we assume that neutrino mass eigenstates arrive at the Earth and no neutrino oscillations take place between the supernova envelope and the surface of the Earth. This can either be justified by the adiabaticity condition for the propagation within the supernova, making mass eigenstates emerge from it, or by decoherence of neutrino oscillations between the surface of the supernova and the Earth. In both cases, Eq. (13) can be split into two independent factors

without interference terms. The issue of wave packet decoherence has, for example, been addressed in Refs. [47, 48, 49, 50, 51, 52]. It has been found that neutrino oscillations vanish for neutrino propagation over distances much larger than the coherence length of the neutrino oscillations. This means that for $L > L_{ab}^{\text{coh}} \propto \sigma E^2 / \Delta m_{ab}^2$ the L/E -dependent interference terms produced by the superposition of the mass eigenstates m_a and m_b in the neutrino oscillation formulas are averaged out. The quantity σ corresponds to a wave packet width determined by the production and detection processes [48, 50]. Since for supernova neutrinos the distance of the propagation is especially large, it is plausible to assume that this averaging takes place and neutrino oscillations vanish by natural decoherence. In other words, the different group velocities of the wave packets of different mass eigenstates combine with dispersive effects such that the overlap of the mass eigenstates is gradually reduced to zero by a factor of $\exp(-[l/L_{ab}^{\text{coh}}]^2)$ in the neutrino oscillation formulas. Hence, for $L > L_{ab}^{\text{coh}}$ the mass eigenstates arrive separately and the coherent transition amplitude in Eq. (12) is split up into two parts to be summed over incoherently (see, *e.g.*, Ref. [51]), having the same effect as the adiabatic transition within the supernova separating the flavor states into mass eigenstates. Thus, it is reasonable to assume that mass eigenstates arrive at the surface of the Earth even for non-adiabatic transitions within the supernova.

Finally, in our numerical analysis, we assume Super-Kamiokande-like water-Cherenkov detectors, *i.e.*, a 32 kt fiducial mass (for supernova neutrinos) Super-Kamiokande detector and a 1 Mt fiducial mass (for solar neutrinos) Hyper-Kamiokande detector. We choose 30 energy bins between the threshold energy 5 MeV and 70 MeV, since above 70 MeV the number of events is rather low. Furthermore, we assume a realistic energy resolution implemented with Gaussian energy smearing with a smearing width proportional to \sqrt{E} such that we have an energy resolution of about 15 % at 10 MeV [44].

5. A neutrino oscillation tomography model

We now introduce and discuss a simple model used for supernova neutrino tomography. As shown in Fig. 4, we assume at least two baselines ending at detectors with similar statistics and systematics, such as Super-Kamiokande-like water-Cherenkov detectors. In order to measure

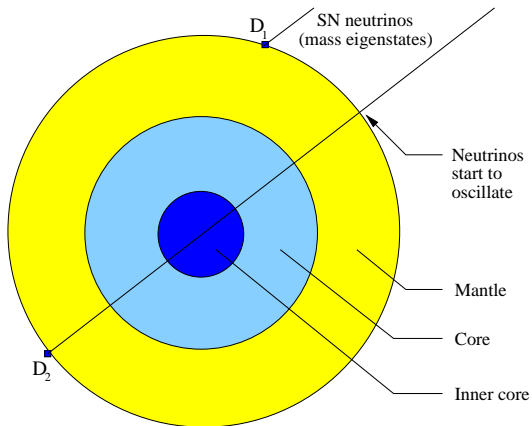


Figure 4. The minimal required setup for supernova neutrino tomography with at least two baselines, one of which is ending at the surface of the Earth at the detector D_1 , the other one is going through the Earth's core (or even the Earth's inner core) to the detector D_2 . In general, we assume that the neutrinos arrive as mass eigenstates at the detector D_1 and start to oscillate when they enter the Earth's interior.

the reference spectrum of the supernova neutrinos, the neutrinos detected at the detector D_1 must not cross the Earth. If we want to obtain information on the Earth's core, then the second detector D_2 needs to observe the supernova neutrinos with a baseline crossing the Earth's core with a sufficient length. The probability to have such a configuration depends upon the location of the supernova in our Galaxy, the time of the day at which the burst arrives at the Earth, and the position of the detectors D_1 and D_2 themselves.

For example, if we consider a supernova located in the galactic center and the detectors placed in Japan and the USA⁷, then, following Ref. [18], one obtains that the probability to find the required setup is around 25 % and 10 % along a day for neutrinos crossing the core and the inner core, respectively. Thus, although this configuration would not work out for many locations of a supernova in the galactic plane, it would be quite likely for a supernova being in the region of the galactic center.

Further on, we assume that the detector D_1 is at least as good as the detector D_2 , which means that the statistics is limited by D_2 , and D_1 measures the reference flux $\Phi_{\bar{\nu}_e}^{D_1}$ with sufficient precision. For the neutrino oscillation parameters we choose $\theta_{12} = 32.9^\circ$, $\theta_{13} = 5^\circ$, $\theta_{23} = 45^\circ$, $\Delta m_{21}^2 = 5.0 \cdot 10^{-5} \text{ eV}^2$, $\Delta m_{32}^2 = 2.5 \cdot 10^{-3} \text{ eV}^2$, and $\delta_{\text{CP}} = 0$ [54,55,56,57,58], *i.e.*, a normal mass hierarchy. Matter effects on supernova neutrinos in the Earth are discussed in detail in Ref. [18], where it is also demonstrated that Earth matter effects would be suppressed for solutions other than the MSW LMA solution. In addition, for detecting antineutrinos the Earth matter effects would only be large enough for our application with an inverted mass hierarchy if $|U_{e3}|^2$ is larger than about 10^{-5} [18]. Thus, we specialize on the (not unlikely) case of the MSW LMA solution with a normal mass hierarchy in order to be able to observe Earth matter effects with a sufficient precision. For our application the dominant neutrino oscillation parameters are the solar neutrino oscillation parameters Δm_{21}^2 and θ_{12} , as well as the matter effects depend on $\sin^2 2\theta_{13}$. Later, we will estimate the precision with which we need to know these parameters and we will test the influence of the size of $\sin^2 2\theta_{13}$. Note that we assume mass eigenstates arriving at the surface of the Earth. Therefore, if D_1 and D_2 were identical detectors, a direct comparison of their energy spectra would verify the existence of Earth matter effects immediately. For detectors of different types fits of the energy spectra would supply similar information in an indirect way.

⁷For instance, one possible site for the UNO proposal would be the WIPP in Carlsbad, New Mexico, USA [53].

For the modeling of the matter density profile we choose the Preliminary Reference Earth Model (PREM) profile [59, 60], as it is shown in Fig. 5, and approximate it by layers of con-

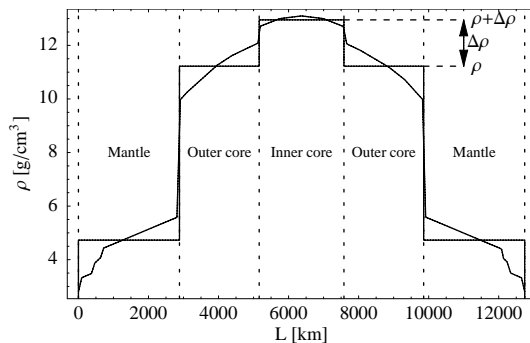


Figure 5. The model for the Earth’s matter density profile used in the calculations (step function) and the PREM matter density profile as function of the path length along the baseline shown in Fig. 4. The quantities which we are interested in are the average outer core matter density ρ and the matter density jump $\Delta\rho$ between average inner and outer core densities, as it is shown in this figure.

stant average matter densities. A baseline with a maximum length of twice the Earth radius then crosses the following layers in this order: mantle, outer core, inner core, outer core, mantle. Since substantial knowledge is provided by geophysics about the Earth’s mantle, we assume its matter density to be known with a sufficient precision. For such a baseline the interesting quantities to measure are the average outer core matter density ρ and the matter density jump $\Delta\rho$ to the average inner core matter density, as illustrated in Fig. 5. This is slightly different to what is known from seismic wave geophysics, since there the density jumps of the actual matter densities at the mantle-core and outer-inner core boundaries are better known. However, since neutrino oscillations are not sensitive to matter densities at individual points, but essentially to the integral of the matter density and the length scale

the neutrinos are traveling through [61], they are more appropriate to measure average matter densities.

The introduced model allows to estimate what could be learned from the neutrinos of a supernova explosion about the Earth's interior. The actual situation, however, such as the number of detectors with baselines through the Earth, their size, the knowledge on the neutrino oscillation parameters, systematics, *etc.*, can only be implemented after the next observed supernova explosion. Our discussion here serves only the purpose of demonstrating that such studies are feasible.

6. Results

Based on the modeling in the last section, we present results, which could be provided by a single supernova. Our analysis is performed with a standard χ^2 technique using [62]

$$\chi^2 \equiv 2 \sum_{i=1}^n \left(x_i^{\text{ref}} - x_i + x_i \log \frac{x_i}{x_i^{\text{ref}}} \right), \quad (26)$$

where n is the number of energy bins, x_i^{ref} is the reference event rate in the i th bin for the true parameters, and x_i is the measured/varied event rate in the i th bin. The errors quoted are read off at the 2σ confidence level – depending on the problem for one or two degrees of freedom. For two degrees of freedom we also take into account the two-parameter correlations. However, we assume that the effects of the systematics are negligible, *i.e.*, the systematical errors are not larger than the statistical errors and the systematics is well understood. This assumption should be reasonable at the time when this application could become relevant.

The most likely case to observe the Earth's core with supernova neutrinos are baselines crossing the Earth's outer core, but not the Earth's inner core, *i.e.*, baselines between about 10,670 km and 12,510 km. Assuming the mantle properties to be known quite well from geophysics, one may then measure the average (outer) core matter density (about 11.4 g/cm³). As a result of the analysis for the scenario S1 in Tab. 1, it turns out that one could measure this core matter density with a baseline just touching the inner core

($L \simeq 12,510$ km) with about 9 % precision with a Super-Kamiokande-like detector and 1.3 % precision with a Hyper-Kamiokande-like detector. We find a rather small dependence on the baseline as long as $L \gtrsim 11,250$ km. For $L \simeq 11,250$ km we still find precisions of 16.5 % (Super-Kamiokande) and 2.5 % (Hyper-Kamiokande), which are growing with an increasing baseline length. The reason for the weak baseline dependence comes from the geometry of the problem, which demonstrates that above a certain threshold the traversed core fraction is rather large, but hardly changes if the total baseline length is further increased. Thus, we will further on not discuss the baseline dependence, since it turns out to be negligible close to the maximal traversed core/inner core distance.

A somewhat more sophisticated application is the combined measurement of the outer and inner core matter densities in the two-parameter model introduced in the last section, *i.e.*, Figs. 4 and 5. In Fig. 6, the results of this analysis without systematical errors and uncertainties are shown in the ρ - $\Delta\rho$ -plane for Super-Kamiokande- and Hyper-Kamiokande-like detectors for the scenario S1 in Tab. 1. One can read off the (absolute) errors at the 2σ confidence level such as shown in this figure. A Super-Kamiokande-like detector cannot verify the inner core, which can be seen in the contours crossing the inner core sensitivity line, *i.e.*, the line $\Delta\rho \equiv 0$. Furthermore, the 3σ contour is rather extensive and cut-off in the upper left corner. Therefore, it is not well-suited for density measurements of the inner core. However, a Hyper-Kamiokande-like detector can clearly observe and verify the inner core even at the 99 % confidence level. Furthermore, quite precise measurements of ρ and $\Delta\rho$ are possible. The relative error for ρ is about 3.1 % and for $\Delta\rho$ about 59 % (2σ confidence level).

As we have indicated in Sec. 4, the supernova parameter scenarios in Tab. 1 other than the scenario S1 perform somewhat worse in the measurement of the parameters ρ and $\Delta\rho$. In addition, degenerate solutions appear at the 2σ confidence level, *i.e.*, different solutions in the parameter space can be fit to the results of the measurement at the considered confidence level. In Tab. 2, we show the errors for the measurement

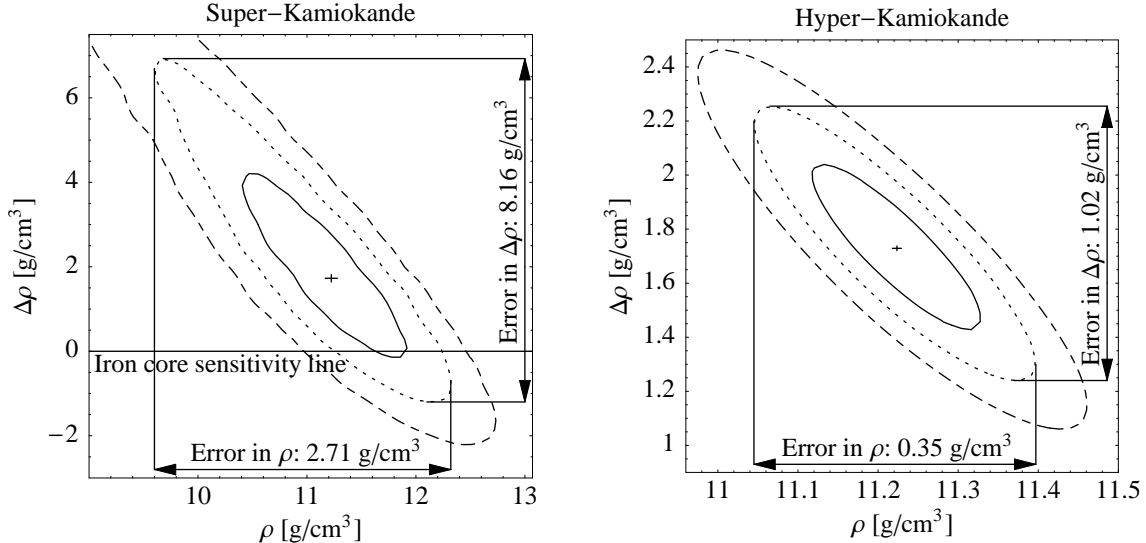


Figure 6. The 1σ , 2σ , and 3σ contours of the χ^2 -function for a measurement of ρ and $\Delta\rho$ for a Super-Kamiokande-like (left-hand plot) and Hyper-Kamiokande-like (right-hand plot) detector and the scenario S1 in Tab. 1 without uncertainties and systematical errors. For the detectors, we use the ones described at the end of Sec. 4. The errors from statistics and correlations are read off at the arrows in the figures. In order to find evidence for the existence of the inner core (the iron core), the contour of the respective confidence level must not cut the inner core sensitivity line corresponding to $\Delta\rho \equiv 0$. This line can only be seen in the left-hand plot. In addition, in the left-hand plot, degenerate solutions are, in principle, present at the 2σ confidence level, which are, however, out of the plot range.

of ρ and $\Delta\rho$ for the Super-Kamiokande detector. It clearly reflects the behavior expected in Sec. 4 and it demonstrates that large values of ξ and τ_E as well as different values for the η 's of the different flavors give the best results. It also shows that the scenario S1 is one of the the most conservative choices of the scenarios for which the tomography application would work. In addition, note that degenerate solutions are in many solutions present due to the energy resolution function of the detector. It turns out that a somewhat higher $\langle E_{\bar{\nu}_e} \rangle$ can improve the results, because it supports the high-energy tail in the spectrum where matter effects are largest.

The results from this measurement cannot be directly compared with the geophysical results, because in seismic wave geophysics the matter density jumps are much easier accessible than the average matter densities. For example, the matter density jump between the outer and inner

cores is believed to be about $(0.55 \pm 0.05) \text{ g/cm}^3$ (see, *e.g.*, Refs. [63, 64, 65, 66]). Translated to the 2σ confidence level, this corresponds to the same order of magnitude as the Hyper-Kamiokande measurement of about 59 % precision. However, the average matter density is much harder to access in geophysics and can only be estimated by the long periodic seismic eigenmodes with uncertainties increasing with depth [23]. The precision on the average matter density of about 3 % from neutrino physics as well as the measurement of the average matter density jump $\Delta\rho$ could help to understand and complement the geophysical information.

Finally, one could consider more than one baseline. If more than one detector observes a supernova through the Earth's core or the inner core, then the potential of this technique would be improved. However, the probability for a single detector to have a baseline through the core is al-

Scenario	ξ	τ_E	$\eta_{\bar{\nu}_e}$	$\eta_{\bar{\nu}_\mu}$	$\delta\rho$	$\delta(\Delta\rho)$	Degs
S1	1.0	1.4	0	0	2.7	8.2	Yes
S2	1.0	1.2	0	0	6.7	17.5	Yes
S3	0.5	1.4	0	0	$\gtrsim 8$	$\gtrsim 21$	Yes
S4	0.5	1.2	0	0	$\gtrsim 12$	$\gtrsim 30$	Yes
S5	1.2	1.4	0	0	2.3	7.0	No
S6	1.2	1.2	0	0	5.0	12.5	Yes
S7	1.0	1.4	3	1	2.0	5.9	No
S8	1.0	1.2	3	1	3.7	10.3	Yes
S9	1.2	1.4	3	1	1.7	5.3	No
S10	1.2	1.2	3	1	3.1	9.1	Yes

Table 2

The different supernova parameter scenarios from Tab. 1 and the absolute errors $\delta\rho$ and $\delta(\Delta\rho)$ (in g/cm^3) for the measurement of ρ and $\Delta\rho$, respectively, at the 2σ confidence level with a Super-Kamiokande-like detector. In addition, the appearance of degenerate solutions (Degs) at the 2σ confidence level is indicated (for Super-Kamiokande).

ready quite low, which means that more detectors would mainly increase the probability that one has an appropriate baseline. Thus, we have in this paper focused on the case of one baseline through the Earth. If really more than one baseline went through the core, then the statistics of the overall measurement would be improved and the result could be estimated by a scaling of the detector. Having one large detector and one baseline corresponds in this application to different detectors at similar positions with their fiducial masses adding up to the one of the single detector.

7. Uncertainties

So far, we have taken into account for our analysis only the statistical errors and the larger two-parameter-correlation. Once illustrated the advantages of our procedure, we now discuss the influence of uncertainties on the measurements of the parameters. We do this separately, because the sensitivity to the parameter extraction, in particular, to the astrophysical parameters, depends significantly upon the model considered.

In order to discuss the influence of uncertainties on the measurements, we estimate the precision to which the leading neutrino oscillation parameters Δm_{21}^2 and θ_{12} have to be known for

the measurement and we vary them until we observe an effect which is as large as the error of the measurement of ρ or $\Delta\rho$. It turns out that these leading parameters have to be known with about 1 % precision for the Super-Kamiokande-like measurements and with about 0.2 % precision for the Hyper-Kamiokande-like measurements. These precisions should be obtainable on the typical timescales of galactic supernova explosions.

The parameter $\sin^2 2\theta_{13}$ also has some influence on the matter effects. For small values, however, the (three-flavor) neutrino oscillations reduce to two two-flavor neutrino oscillation schemes one describing the solar neutrino oscillations and the other one the atmospheric neutrino oscillations. We tested the influence of this parameter on our applications and we found that it can be safely neglected as long as $\sin^2 2\theta_{13}$ is not too large. Only at the CHOOZ bound minor corrections much smaller than the error of our measurements have to be performed. However, this bound will be reduced in the short term future by planned superbeamed and neutrino factory experiments (for a summary of expected boundaries see, for example, Ref. [67]).

One of the most important uncertainties in this measurement comes from measuring the electron antineutrinos only. It can be easily seen from

Param.	SuperK	HyperK	Effects
$E_{\bar{\nu}_e}^{\text{tot}}$	$\sim 5\%$	$\sim 1\% - 2\%$	$\lesssim 1\%$
$E_{\bar{\nu}_\mu}^{\text{tot}}$	$\sim 100\%$	$\sim 10\%$	large
$\langle E_{\bar{\nu}_e} \rangle$	$\sim 5\%$	$\sim 1\% - 2\%$	$\lesssim 5\% - 10\%$
$\langle E_{\bar{\nu}_\mu} \rangle$	$\sim 10\%$	$\sim 1\% - 2\%$	$\lesssim 5\%$

Table 3

The uncertainties on the supernova parameters extracted from the Super-Kamiokande (SuperK) or Hyper-Kamiokande (HyperK) measurements from Refs. [45, 46] and their estimated effects on our parameter measurements as percentage corrections.

Eq. (20) that the extraction of the fluxes of the mass eigenstates from the flux of the electron antineutrino flavor involves assumptions about the supernova parameters, which are entering by the flux ratio f_R . Thus, if only the electron antineutrinos from the supernova can be measured, then the tomography problem will be closely connected to the determination of the supernova parameters at a detector on the surface of the Earth. Estimates for the precision of the supernova parameter determinations depend on the initial values considered. Thus, the more different the $\bar{\nu}_e$ and $\bar{\nu}_\mu$ spectra are formed in a supernova explosion, the stronger the oscillation effects are, and therefore, the better one can measure the neutrino temperatures and luminosities. As an example, we show in Tab. 3 the sensitivities obtained in Refs. [45, 46].⁸ In addition, this table shows the estimated influences on the determination of our parameters from a variation of the supernova parameters in the numerical evaluation. The reason for the similar percentage effects for Super-Kamiokande and Hyper-Kamiokande is the parallel scaling of both problems. It is interesting to observe that none of the supernova parameters has a strong influence on the tomography problem except from the overall energy of the muon antineutrinos $E_{\bar{\nu}_\mu}^{\text{tot}}$. One can show that this parameter has to be known up to about 20 % for the Super-Kamiokande measurement and 3 % - 4 % for the Hyper-Kamiokande measurement in

order not to have strong effects on the tomography problem. However, this precision cannot be achieved by measuring the electron flavor only. Altogether, either $E_{\bar{\nu}_\mu}^{\text{tot}}$ needs to be measured by different experiments or the fluxes of the muon and tau antineutrinos need to be determined simultaneously with the electron antineutrino flux, making the supernova parameters entirely drop out. This can be seen in Eq. (17), which allows the reconstruction of all mass fluxes at the detector D_1 if all flavor fluxes are measured.

Another issue in the discussion of uncertainties is the parameter Y_e in Eq. (6) relating the number of electrons to the number of nucleons. Since the Earth matter effects in neutrino oscillations actually depend on the electron density and not on the matter density directly, additional uncertainties enter in the conversion of these two quantities by the parameter Y_e . We assumed $Y_e = 0.5$ in our calculations, but for different materials this parameter can differ somewhat from this value – especially in the inner core. In order to find out the material in each matter density layer, one may prefer to measure the electron density instead of the matter density. However, since in each layer these quantities are proportional to each other, the problem does not change by using the matter density and the electron density can be easily calculated.

So far, we have assumed the average mantle matter density to be known exactly. In fact, matter density uncertainties up to 5 % have been documented (for a summary, see, *e.g.*, Ref. [68]). Testing these uncertainties, even the conservative choice of a 5 % uncertainty on the average mantle density is no problem for the Super-Kamiokande

⁸The results in this reference were obtained for $\eta_{\bar{\nu}_e} = 2.6$, $\eta_{\bar{\nu}_\mu} = 0$, and $\xi = 0.5$. In this paper, however, we have used slightly different parameter values for which the precisions on the supernova parameters in Tab. 3 would become somewhat worse by about a factor of two.

detector. However, for the Hyper-Kamiokande detector, it should not be larger than about 2 %. Because of a partial averaging out of the uncertainties for the very long baselines considered in this paper, this uncertainty should be quite realistic [61].

Another source of uncertainty has to do with the knowledge of the location of a supernova, since it may affect the baseline length. In a future core-collapse supernova in our Galaxy, the electromagnetic radiation can be obscured by dust in the interstellar space. In this case, the localization of the supernova can be done by studying neutrino-electron forward scattering. A conservative estimate leads to restrict the supernova direction with an error of about 5° in the Super-Kamiokande detector [35]. However, with the increase of statistics expected in a megaton detector, this uncertainty would be reduced. On the other hand, complementary information could be inferred by the triangulation method [35], namely the direct measurement of the delay of the signal to the two detectors. Therefore, we consider that this small error would not imply a significant change in the long baselines that we are dealing with, since even for a 5° directional uncertainty the baseline length of about 12,700 km does not change very much.

8. Summary and conclusions

We have discussed the possibility to use the neutrinos from a future galactic supernova explosion to obtain additional information on the Earth's core. First, we have summarized geophysical aspects and unknowns of the Earth's core. Then, we have investigated core-collapse supernovae as potential neutrino sources for a snapshot of the Earth's interior. Next, we have discussed the neutrino propagation from the production to the detection in detail, where we have especially focused on Earth matter effects on the neutrino oscillations of the supernova neutrinos. We have also put these effects into the context of the supernova parameters, *i.e.*, temperatures and deviation from energy equipartition. Furthermore, we have stressed the importance of supernova neutrinos arriving at the surface of the Earth as mass eigen-

states for this technique, which we have also supported by a discussion of decoherence of neutrino oscillations. We have shown that we need one detector on the surface of the Earth on the side towards the supernova, and another one in the shadow of the Earth's core. For the most likely scenario of not crossing the Earth's inner core, we have shown that the Earth's average core matter density could be determined up to 9 % with a Super-Kamiokande-like and 1.3 % with a Hyper-Kamiokande-like detector (all errors at the 2σ confidence level). In addition, for a less likely two-parameter measurement of the outer and inner core matter densities, Hyper-Kamiokande could verify the existence of the inner core at the 3σ confidence level and measure the outer core matter density with a precision of about 3.1 %, as well as the density jump between outer and inner core matter densities with a precision of about 59 %. The latter error is comparable to seismic wave geophysics, where, however, not the difference between the average matter densities, but the matter density jump at the outer-inner core boundary is measured. Thus, neutrino physics could provide complementary information to geophysics. However, the quoted numbers for the precisions depend on the supernova parameter values, indirectly determined by the on-the-surface measurement, and are in some cases better, in others worse. Thus, the actual precisions will not be known before the supernova goes off. In general, we find that the more muon and tau neutrinos are produced, the larger the temperature difference between the different flavors is, and the more different the degeneracy parameters for the different flavors are, the better the application works. Finally, we have discussed several uncertainties to these measurements and we have found that especially the determination of the total muon antineutrino energy of the supernova causes problems to our method. However, measuring not only electron antineutrinos, but also the other two flavors could completely eliminate the dependence on the supernova parameters. Furthermore, the leading solar neutrino parameters have to be known with sufficient precision, which is about 0.2 % for Hyper-Kamiokande-like measurements. In summary, supernova neutrino tomog-

raphy could be a nice additional payoff of existing or planned detectors if all of the prerequisites can be met at the time when the next supernova explodes.

Acknowledgments

We would like to thank Heiner Igel for useful discussions and Evgeny Kh. Akhmedov and John F. Beacom for valuable comments.

This work was supported by the Swedish Foundation for International Cooperation in Research and Higher Education (STINT) [T.O.], the Wenner-Gren Foundations [T.O.], the Swedish Research Council (Vetenskapsrådet), Contract No. 621-2001-1611 [T.O.], the Magnus Bergvall Foundation (Magn. Bergvalls Stiftelse) [T.O.], the “Deutsche Forschungsgemeinschaft” (DFG) [R.T.], the “Studiens-tiftung des deutschen Volkes” (German National Merit Foundation) [W.W.], and the “Sonderforschungsbereich 375 für Astro-Teilchenphysik der Deutschen Forschungsgemeinschaft” [M.L., T.O., and W.W.].

REFERENCES

1. L.V. Volkova and G.T. Zatsepin, *Bull. Phys. Ser.* 38 (1974) 151.
2. A.D. Rújula et al., *Phys. Rep.* 99 (1983) 341.
3. T.L. Wilson, *Nature* 309 (1984) 38.
4. G.A. Askar'yan, *Usp. Fiz. Nauk* 144 (1984) 523, [*Sov. Phys. Usp.* 27 (1984) 896].
5. A. Borisov, B. Dolgoshein and A. Kalinovskii, *Yad. Fiz.* 44 (1986) 681, [*Sov. J. Nucl. Phys.* 44 (1987) 442].
6. A. Nicolaidis, M. Jannane and A. Tarantola, *J. Geophys. Res.* 96 (1991) 21811.
7. H.J. Crawford et al., *Proc. of the XXIVth International Cosmic Ray Conference* (University of Rome) (1995) 804.
8. C. Kuo et al., *Earth Plan. Sci. Lett.* 133 (1995) 95.
9. P. Jain, J.P. Ralston and G.M. Frichter, *Astropart. Phys.* 12 (1999) 193, hep-ph/9902206.
10. V.K. Ermilova, V.A. Tsarev and V.A. Chechin, *Bull. Lebedev Phys. Inst.* NO.3 (1988) 51.
11. V.A. Chechin and V.K. Ermilova, *Proc. of LEWI'90 School*, Dubna (1991) 75.
12. T. Ohlsson and W. Winter, *Phys. Lett.* B512 (2001) 357, hep-ph/0105293.
13. T. Ohlsson and W. Winter, *Europhys. Lett.* 60 (2002) 34, hep-ph/0111247.
14. A.N. Ioannisian and A.Y. Smirnov, hep-ph/0201012.
15. S. Mikheyev and A. Smirnov, *Yad. Fiz.* 42 (1985) 1441, [*Sov. J. Nucl. Phys.* 42 (1985) 913].
16. S. Mikheyev and A. Smirnov, *Nuovo Cimento C* 9 (1986) 17.
17. L. Wolfenstein, *Phys. Rev.* D17 (1978) 2369.
18. C. Lunardini and A.Y. Smirnov, *Nucl. Phys.* B616 (2001) 307, hep-ph/0106149.
19. K. Takahashi and K. Sato, *Phys. Rev.* D66 (2002) 033006, hep-ph/0110105.
20. K. Takahashi, M. Watanabe and K. Sato, *Phys. Lett.* B510 (2001) 189, hep-ph/0012354.
21. K. Aki and P.G. Richards, *Quantitative Seismology - Theory and Methods* (W. H. Freeman, San Francisco, 1980), Vol. 1, 2.
22. T. Lay and T.C. Wallace, *Modern Global Seismology* (Academic Press, New York, 1995).
23. H. Igel, private communication.
24. G. Steinle-Neumann, L. Stixrude and R.E. Cohen, physics/0204055.
25. G.G. Raffelt, *Nucl. Phys. Proc. Suppl.* 110 (2002) 254, hep-ph/0201099.
26. H.T. Janka and W. Hillebrandt, *Astron. Astrophys.* 224 (1989) 49.
27. H.T. Janka and W. Hillebrandt, *Astron. Astrophys. Suppl.* 78 (1989) 375.
28. P.M. Giovanoni, D.C. Ellison and S.W. Bruenn, *Astrophys. J.* 342 (1989) 416.
29. M.T. Keil, G.G. Raffelt and H.T. Janka, astro-ph/0208035.
30. H.T. Janka, In *Vulcano 1992, Proceedings, Frontier objects in astrophysics and particle physics* 345-374.
31. T. Totani et al., *Astrophys. J.* 496 (1998) 216, astro-ph/9710203.
32. G.G. Raffelt, *Astrophys. J.* 561 (2001) 890.

33. R. Buras et al., astro-ph/0205006.
34. A. Mezzacappa et al., Phys. Rev. Lett. 86 (2001) 1935, astro-ph/0005366.
35. J.F. Beacom and P. Vogel, Phys. Rev. D60 (1999) 033007, astro-ph/9811350.
36. E.K. Akhmedov, C. Lunardini and A.Y. Smirnov, Nucl. Phys. B643 (2002) 339, hep-ph/0204091.
37. A.S. Dighe and A.Y. Smirnov, Phys. Rev. D62 (2000) 033007, hep-ph/9907423.
38. A.Y. Smirnov, D.N. Spergel and J.N. Bahcall, Phys. Rev. D49 (1994) 1389, hep-ph/9305204.
39. M. Kachelrieß et al., Phys. Rev. D65 (2002) 073016, hep-ph/0108100.
40. T. Ohlsson and H. Snellman, Phys. Lett. B474 (2000) 153, hep-ph/9912295, B480 (2000) 419(E).
41. E.K. Akhmedov, Yad. Fiz. 47 (1988) 475, [Sov. J. Nucl. Phys. 47 (1988) 301].
42. S.T. Petcov, Phys. Lett. B434 (1998) 321, hep-ph/9805262, B444 (1998) 584(E).
43. E.K. Akhmedov, Nucl. Phys. B538 (1999) 25, hep-ph/9805272.
44. J.N. Bahcall, P.I. Krastev and E. Lisi, Phys. Rev. C55 (1997) 494, nucl-ex/9610010.
45. V. Barger, D. Marfatia and B.P. Wood, Phys. Lett. B547 (2002) 37, hep-ph/0112125.
46. H. Minakata et al., Phys. Lett. B542 (2002) 239, hep-ph/0112160.
47. C. Giunti, C.W. Kim and U.W. Lee, Phys. Rev. D44 (1991) 3635.
48. C. Giunti and C.W. Kim, Phys. Rev. D58 (1998) 017301, hep-ph/9711363.
49. W. Grimus, P. Stockinger and S. Mohanty, Phys. Rev. D59 (1999) 013011, hep-ph/9807442.
50. C.Y. Cardall, Phys. Rev. D61 (2000) 073006, hep-ph/9909332.
51. M. Lindner, T. Ohlsson and W. Winter, Nucl. Phys. B622 (2002) 429, astro-ph/0105309.
52. C. Giunti, J. High Energy Phys. 11 (2002) 017, hep-ph/0205014.
53. The UNO Collaboration web page, <http://superk.physics.sunysb.edu/nngroup/uno/main.html>
54. J.N. Bahcall, M.C. Gonzalez-Garcia and C. Peña-Garay, J. High Energy Phys. 07 (2002) 054, hep-ph/0204314.
55. CHOOZ Collaboration, M. Apollonio et al., Phys. Lett. B420 (1998) 397, hep-ex/9711002.
56. CHOOZ Collaboration, M. Apollonio et al., Phys. Lett. B466 (1999) 415, hep-ex/9907037.
57. CHOOZ Collaboration, C. Bemporad, Nucl. Phys. B (Proc. Suppl.) 77 (1999) 159.
58. Super-Kamiokande Collaboration, T. Toshito, hep-ex/0105023.
59. F.D. Stacey, Physics of the Earth, 2 ed. (Wiley, 1977).
60. A.M. Dziewonski and D.L. Anderson, Phys. Earth Planet. Inter. 25 (1981) 297.
61. B. Jacobsson et al., Phys. Lett. B532 (2002) 259, hep-ph/0112138.
62. Particle Data Group, D.E. Groom et al., Eur. Phys. J. C15 (2000) 1, <http://pdg.lbl.gov/>.
63. G. Masters and P. Shearer, J. Geophys. Res. 95 (1990) 21,619.
64. P. Shearer and G. Masters, Geophys. J. Int. 102 (1990) 491.
65. M. Ishii and J. Tromp, Science 285 (1999) 1231.
66. G. Masters, G. Laske and F. Gilbert, Geophys. J. Int. 143 (2000) 478.
67. P. Huber, M. Lindner and W. Winter, Nucl. Phys. B645 (2002) 3, hep-ph/0204352.
68. S.V. Panasyuk, REM (Reference Earth Model) web page, <http://cfauvcs5.harvard.edu/lana/rem/index.htm>